논문 2007-44TC-3-2

개구면 결합 공진기 급전 마이크로스트립 방향성결합기 해석 및 설계

(Analysis and Design Theory of Aperture-Coupled Cavity-Fed Back-to-Back Microstrip Directional Coupler)

남 상 호*, 장 국 현*, 남 경 민*, 이 장 환*, 김 철 언*, 김 정 필**

(Sang Ho Nam, Guk hyun Jang, Kyung Min Nam, Jang Hwan Lee, Chul Un Kim, and Jeong Phill Kim)

요 약

개구면 결합 공진기 급전 마이크로스트립 방향성결합기의 특성을 해석하였고, 최적 설계를 위한 효율적인 설계 이론을 제시한다. 이러한 목적을 위해 단순하고도 정확한 등가 회로를 도출하였고, 도출된 등가 회로를 바탕으로 결합기의 설계 수식을 유도하였다. 여러 구조적 설계 변수를 결정하기 위해, 유전 알고리즘과 Nelder-Mead 방법에 기반한 진화적 이종 최적화 방법을 사용하였으며, 제안한 설계 방식과 최적화 설계 방법의 타당성을 검증하기 위해 10 dB 방향성 결합기를 설계, 제작하였다. 측정된 결합기의 결합 계수는 3 GHz 에서 10.3 dB 였고, 반사계수와 isolation은 각각 31.8 dB 와 30.5 dB 였다. 또한 출력단과 결합단 사이에 90° 위상 차이를 보였다. 측정치와 설계치의 일치도는 제안한 해석 방법과 등가 회로 및 최적화 설계의 타당성을 검증해 준다.

Abstract

An analysis and design theory of an aperture-coupled cavity-fed back-to-back microstrip directional coupler is presented for the efficient and optimized design. For this purpose, an equivalent network is developed, and simple but accurate calculations of circuit element values are described. Design equations of the coupler are derived based on the equivalent circuit. In order to determine various structural design parameters, the evolutionary hybrid optimization method based on the genetic algorithm and Nelder-Mead method is invoked. As a validation check of the proposed theory and optimized design method, a 10 dB directional coupler was designed and fabricated. The measured coupling was 10.3 dB at 3 GHz, and the return loss and isolation were 31.8 dB and 30.5 dB, respectively. The directional coupler also showed very good quadrature phase characteristics. Good agreements between the measured and the design specifications fully validate the proposed network analysis and design procedure.

Keywords : Aperture-coupling, cavity-feed, directional coupler, microstrip circuit, hybrid optimization,

I. Introduction

The need for heat sink and structural support for active circuits, especially in active phased array antenna elements, often requires the use of relatively thick ground plane. Aperture-coupled cavity-fed coupling structure, which enables an electromagnetic wave to propagate without decay (above the cut off) in waveguide sections in thick ground plane, is of interest in multilayer microwave and millimeter wave circuits as an efficient means of electrical

* 학생회원, ** 정회원, 중앙대학교
(School of Electrical and Electronic Engineering Chung-Ang University)

※ 이 논문은 2006학년도 중앙대학교 학술연구비 지원에 의한 것임.
접수일자: 2007년2월22일, 수정완료일: 2007년3월14일

interconnection between layers. In addition to the better electrical characteristics, it provides much more design flexibility.

Researches on aperture-coupled cavity-fed microstrip couplers have been undertaken[1]-[3], but these are limited to only single coupling section. In order to realize directional coupling characteristics, studies are needed on multi-section coupling structures and efficient design methods. Although the numerical analyses can be applied for the accurate analysis of the aforementioned coupling structures, these have a limitation in design applications where a large number of design parameters are involved. Therefore development of an elaborated equivalent circuit, which is based on an analytic or semi-analytic method, is needed for the optimized computer-aided designs.

This paper presents network analysis and design theory of an aperture-coupled cavity-fed back-to-back microstrip directional coupler, where two coupling sections are connected by stepped impedance microstrip lines. An equivalent network is developed for the optimized design purpose, and simple but accurate calculation of circuit element values is described. Based on this equivalent circuit, design equations of the directional coupler are derived and applied to design directional couplers, where an evolutionary hybrid optimization method based on the genetic algorithm[4] and Nelder-Mead method[5] is invoked to determine the structural parameters.

Ⅱ. Network Analysis and Equivalent Circuit

The geometry of a symmetric aperture-coupled cavity-fed back-to-back microstrip directional coupler is shown in Fig. 1, where two identical sections of aperture-coupled cavity-fed coupling structures are connected with two identical connecting microstrip lines. The bottom and top microstrip lines are chosen as the feed and coupled lines, respectively. The thickness and dielectric constant of microstrip substrates are d and ε_r, respectively. The width of microstrip port line is denoted by W. L_s and W_s are

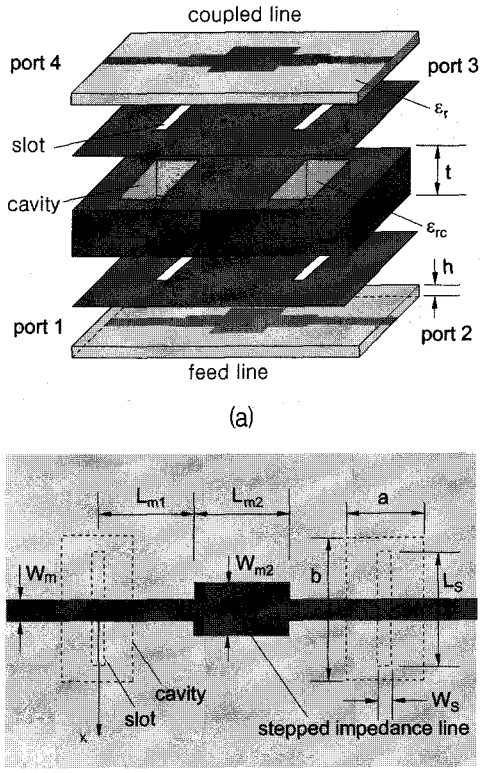

그림 1. 개구면 결합 공진기 급전 등진 구조 마이크로스트립 방향성 결합기의 형태; (a) 3차원모양; (b) 상부모양

Fig. 1. Geometry of aperture-coupled cavity-fed back-to-back microstrip directional coupler; (a) 3 dimensional view; (b) top view

the length and width of the coupling slots, and a, b, and t are the width, height, and thickness of the cavities, respectively. The cavities are filled with a dielectric material with dielectric constant ε_{rc}. In some cases, multiple dielectric sheets can be stacked in the cavities. It is important that the dimensions of slots and dielectric filled waveguide should be chosen to ensure the below resonant mode and the above the cut off mode operations, respectively. As the connecting lines, stepped impedance microstrip lines are introduced, where a uniform line is the special case of stepped impedance lines. A higher degree of design freedom can be provided with the stepped impedance lines. L is the extended length of the feed line. L_1 and W_1 are the length and width of the microstrip stepped impedance line, respectively.

At first, an equivalent circuit of a single coupling section, which consists of two identical microstrip

lines and cavity with two identical coupling apertures, is considered. The equivalent network models developed for an aperture coupled microstrip lines, back to back coupler, and patch antenna [6]-[8] have to be combined and slightly modified for reflecting the effect of aperture coupled cavity in a thick ground plane accurately [9]. In order to facilitate the reader's understanding, the related theories are described briefly.

It is well known that electromagnetic coupling between the microstrip line and aperture in the ground plane can be modeled by an ideal transformer with the help of the reciprocity theorem [10]. The turns ratio n_t is expressed as

$$n_t = \int_S (\bar{e}_s \times \bar{h}_m) \cdot \hat{n}\, dS \tag{1}$$

where S is the aperture area, $\bar{e}_s$ is the aperture electric field which is normalized so that the voltage across the slot center becomes 1 V, $\bar{h}_m$ denotes the magnetic field of a microstrip line under the normalization condition of unit current flow (1 A), and $\hat{n}$ is the outward normal unit vector. Since the aperture electric field is known to be well approximated by $\bar{e}_s = \hat{x} e_{sx}$ with

$$e_{sx} = \frac{\cos(\pi y / L_s)}{\pi \sqrt{(W_s/2)^2 - x^2}} \tag{2}$$

only the y-component magnetic field h_{my} contributes to the above integral. With the following inverse Fourier transform expression of h_{my}:

$$h_{my}(y) = \frac{1}{2\pi} \int_{-\infty}^{\infty} \tilde{h}_{my}(k_y) e^{-jk_y y} dk_y \tag{3}$$

the following expression of n_t can be obtained.

$$n_t = \frac{J_0(W_s \beta_m / 2)}{L_s} \int_{-\infty}^{\infty} \tilde{h}_{my}(k_y) \frac{\cos(k_y L_s/2)}{(\pi/L_s)^2 - k_y^2} dk_y \tag{4}$$

where β_m is the phase constant of microstrip line. With the help of the spectral domain immittance approach [6],[11], the following expression of $\tilde{h}_{my}(k_y)$ $\tilde{h}_{my}(k_y)$ can be obtained under the assumption of only the x-component current flow on the microstrip line:

$$\tilde{h}_{my} = \frac{1}{\cosh(\gamma_d d)} \tilde{G}_{yx}^{HJ} \tilde{J}_{my}(k_y) \tag{5}$$

where $\tilde{G}_{yx}^{HJ}$ denotes the spectral domain Green's function of the y-component magnetic filed due to the x-component current density on microstrip line J_{mx} [6],[11], and $\tilde{J}_{mx}(k_y)$ is the Fourier transform of $J_{mx}(y)$. The following function is well known to approximate the current density on microstrip line:

$$J_{mx}(y) = \frac{1}{\pi \sqrt{(W/2)^2 - y^2}} \tag{6}$$

Looking over the integrand in equation (4), it is not difficult to know that the integrand has no singularity along the real k_y axis, and converges fast as k_y. Therefore n_t can be evaluated numerically without difficulty.

The effect of the complex power flow into the half space with substrate from aperture is represented by the admittance Y_s in the spectral domain as

$$\begin{aligned} Y_s &= -\int_s (m_{sy}^* H_y) dS \\ &= \frac{-1}{4\pi^2 |V_s|^2} \int_{-\infty}^{\infty} \int_{-\infty}^{\infty} \tilde{G}_{xx}^{HM} |\tilde{M}_{sx}|^2 dk_x dk_y \end{aligned} \tag{7}$$

where $\tilde{G}_{xx}^{HJ}$ denotes the spectral-domain Green's function of magnetic field H_{sx} due to the equivalent magnetic current density m_{sx} just above the ground plane, and $\tilde{M}_{sx}$ is the Fourier transform of m_{sx}. With the spectral-domain immittance approach [11] and the Fourier transform relation, $\tilde{G}_{xx}^{HM}$ and $\tilde{M}_x$ are obtained as

$$\tilde{G}_{xx}^{HM} = \frac{-(k_x^2 Y_{TE}^s + k_y^2 Y_{TE}^s)}{k_x^2 + k_y^2} \tag{8}$$

$$\tilde{M}_{sx} = \frac{2\pi}{L_s} \frac{\cos(k_x L_s/2)}{(\pi/L_s)^2 - k_x^2} J_0\left(\frac{W_s |k_y|}{2}\right) \tag{9}$$

where $J_0(.)$ denotes the 1st kind of Bessel function of zero order, and Y_{TE} and Y_{TM} are the input wave admittances for the TE_z and TM_z modes,

respectively. Applying the rectangular-to-polar coordinate transformation and the symmetry property of $\tilde{G}_{xx}^{HJ}$ and $|\tilde{M}_{sx}|^2$, Y_s can be numerically evaluated without difficulty with the help of the contour deformation [12] and asymptotic extraction techniques [13].

The rectangular cavity with two apertures in a thick ground plane can be regarded as two aperture-to-waveguide sections in a back-to-back configuration. Considering the behavior of the y-component magnetic field in the waveguide H_{wy}, the Fourier series is chosen as

$$H_{wy}(x,y)=\sum_{m=1}^{\infty}\sum_{n=0}^{\infty}H_{mn}\sin k_{xm}(x+a/2)\cos k_{yn}(y+b/2) \quad (10)$$

where $k_{xm}=m\pi/a$, $k_{yn}=m\pi/b$, and H_{mn} is the mn-th Fourier coefficient of H_{wy}. With this choice and applying the Parseval's theorem and some algebraic manipulations, Y_{sw}, the input admittance looking into the waveguide from the aperture, is expressed as

$$\begin{aligned} Y_{sw} &= -\int_S (m_{sy}^* H_{wy})dS \\ &= \sum_{m=1}^{\infty}\sum_{n=0}^{\infty}\left\{(n_{nm}^{TE})^2 Y_{mn}^{TE}+(n_{mn}^{TE})^2 Y_{mn}^{TM}\right\} \end{aligned} \quad (11)$$

with

$$(n_{mn}^{TE})^2=\frac{ab}{2\epsilon_n}|(\tilde{M}_{sx})_{mn}|^2\frac{k_{xm}^2}{k_{xm}^2+k_{yn}^2} \quad (12)$$

where $(\tilde{M}_{sx})_{mn}$, the mn-th Fourier coefficients of m_{sx}, is given as

$$(\tilde{M}_{sx})_{mn}=\frac{2\epsilon_n}{ab}\frac{2\pi}{L_s}\frac{\cos(k_x L_s/2)\sin(k_{xm}a/2)}{(\pi/Ls)^2-k_x^2}J_0\left(\frac{W_s|k_y|}{2}\right)\cos\left(\frac{k_{yn}b}{2}\right) \quad (13)$$

and εn = 1 for n = 0 and εn = 2 for n ≠ 0. The expression of $(n_{mn}^{TM})^2$ is the same as that of $(n_{mn}^{TE})^2$ with kxm and kyn interchanged. Each mode of a waveguide can be modeled by the corresponding equivalent transmission line, and n_{mn}^{TE} and n_{mn}^{TM} can be considered as the turns ratios of the equivalent ideal transformers between the slot and the corresponding waveguide mode voltages. A simple equivalent circuit representation can therefore be made. Now since the opposite part can be modeled similarly, the equivalent circuit of a single section coupling structure is obtained as shown in Fig. 2. The equivalent circuit for each transmission line section can be analyzed using the ABCD matrix formulation. From the obtained ABCD matrix, the admittance parameters of the equivalent π-network are obtained by the

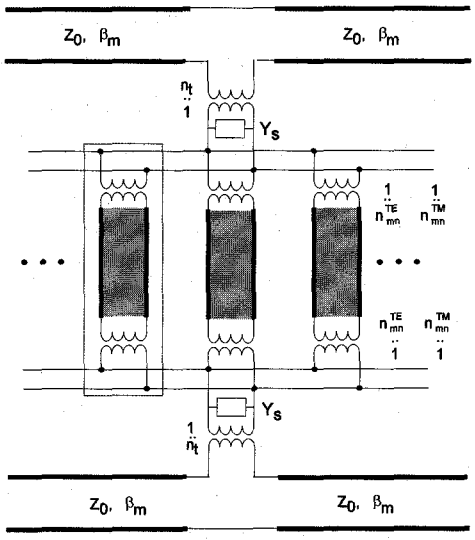

그림 2. 단일 결합 부의 등가회로 모델

Fig. 2. Equivalent circuit representation of a single coupling section.

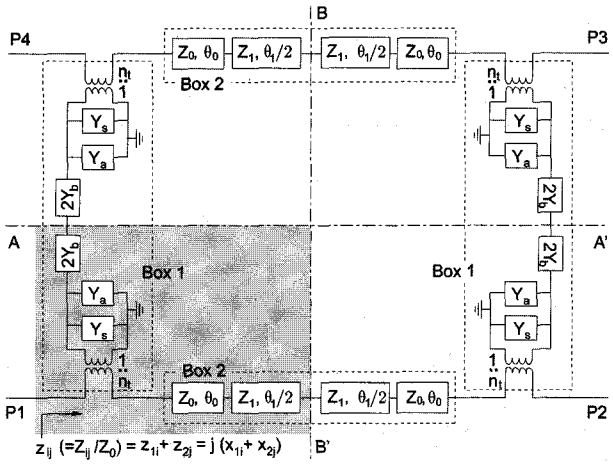

그림 3. 개구면 결합 급전 등진구조 마이크로스트립 방향성 결합기의 등가 회로

Fig. 3. Equivalent circuit of an aperture-coupled cavity-fed back-to-back microstrip directional coupler.

network parameter conversion [14] as shown in the dashed box. All the parallel connected π-networks can be represented by single π-network with admittance parameters Ya and Yb. Therefore the final equivalent network of the directional coupler is obtained as shown in Fig. 3. Even though the radiation loss from coupling slots can be included in the equivalent circuit, it will be ignored for the derivation of coupling condition.

III. Coupling Theory and Design Equations

Now a coupling theory of the proposed directional coupler is considered from the obtained equivalent circuit. The directional coupler is a four port network with two fold symmetry planes (AA' and BB') as shown in Fig. 3. The connecting transmission-line sections are the circuit representation of the extended feed line (electrical line length θ_0) and stepped impedance microstrip line (characteristic impedance Z_1 and electrical length θ_1). Even though uniform line is one candidate of connecting lines, it just the special case of stepped impedance lines.

The scattering parameters can be calculated with the even-odd mode analysis by considering only one-quarter part of the circuit (Fig 3) [14]. Under the assumption of a lossless directional coupler, normalized input impedance z_{ij} (= Z_{ij}/Z_0) can be expressed as $z_{ij} = jx_{ij} = j(x_{1i} + x_{2j})$ where ij = *ee*, *eo*, *oe*, or *oo*, with the following meanings:

ee : AA' is open circuited and BB' open circuited,
eo : AA' is short circuited and BB' open circuited,
oe : AA' is open circuited and BB' short circuited,
oo : AA' is short circuited and BB' short circuited.

With the corresponding reflection coefficient $\Gamma_{ij} = (z_{ij} - 1)/(z_{ij} + 1)$, the scattering parameters of the directional coupler are obtained as

$$S_{11} = (\Gamma_{ee} + \Gamma_{eo} + \Gamma_{oe} + \Gamma_{oo})/4 \quad (14a)$$

$$S_{21} = (\Gamma_{ee} - \Gamma_{eo} + \Gamma_{oe} - \Gamma_{oo})/4 \quad (14b)$$

$$S_{31} = (\Gamma_{ee} - \Gamma_{eo} + \Gamma_{oe} - \Gamma_{oo})/4 \quad (14c)$$

$$S_{41} = (\Gamma_{ee} + \Gamma_{eo} - \Gamma_{oe} - \Gamma_{oo})/4 \quad (14d)$$

Now the conditions of directional coupler are considered. If the port 1 and 4 are chosen as input and isolation ones, respectively, the following conditions can be derived from the matching and isolation conditions (S_{11}=0 and S_{41}=0):

$$x_{ee}x_{eo} = -1 \quad (15a)$$

$$x_{oe}x_{oo} = -1 \quad (15b)$$

Under these matching and isolation conditions, S_{31}/S_{21} is given as

$$\frac{S_{31}}{S_{21}} = \frac{-j(x_{ee} - x_{oe})}{1 + x_{ee}x_{oe}} \quad (16)$$

and the phase difference therefore becomes 90°. This implies that the proposed directional coupler can be used as a quadrature hybrid. Algebraic manipulation of equations (15a) and (15b) yields $(x_{1e} - x_{1o})(x_{ee} + x_{oo}) = 0$. Under the case $x_{1e} \neq x_{1o}$, which is a general case for the directional coupler considered in this paper, the following condition can be obtained

$$x_{ee} + x_{oo} = 0 \quad (17)$$

Using these relations, the coupling factor C (=$|S_{31}|$) can be expressed as a function of x_{ee} only as

$$C^2 = \frac{\left(1 - x_{ee}^2\right)^2}{\left(1 + x_{ee}^2\right)^2} \quad (18)$$

and four different values of x_{ee} are therefore determined for the given coupling factor C as

$$x_{ee} = \pm\sqrt{\frac{1-C}{1+C}} \quad \text{or} \quad \pm\sqrt{\frac{1+C}{1-C}} \quad (19)$$

Fig. 4 shows four different values of x_{ee} with respect to coupling C.

In order to design a directional coupler, four reactance values x_{1e}, x_{1o}, x_{2e}, and x_{2o} should be

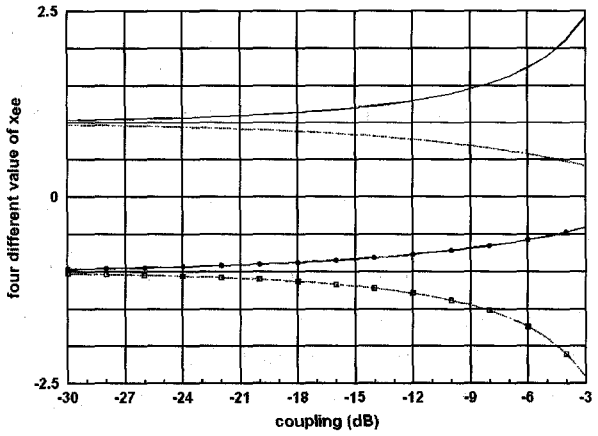

그림 4. 결합량에 따른 4개의 서로 다른 x_{ee} 값들

Fig. 4. Four different values of xee with respect to coupling.

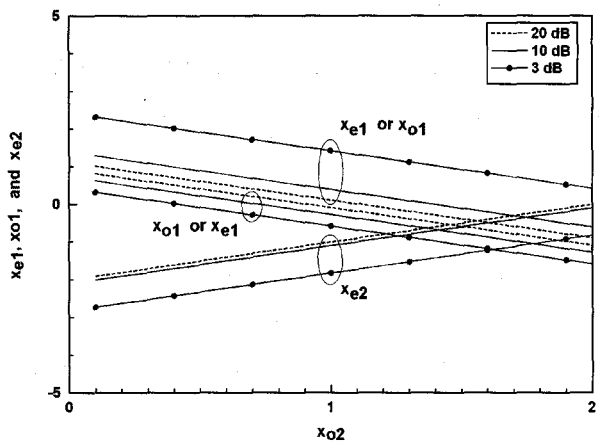

그림 5. x_{o2}에 대한 x_{e1}, x_{o1} 그리고 x_{e2} 의 설계 곡선

Fig. 5. Design curves for x_{e1}, x_{o1}, and x_{e2} as a function of x_{o2}.

determined from the given conditions. In general, the length of the connecting line is order of quarter-wave length, and x_{1e} and x_{1o} are therefore negative and positive, respectively. Fig. 5 shows reasonable sets of x_{1e}, x_{2e}, and x_{2o} for the specified coupling as a function of x_{1o}. Since there are only three conditions (matching, isolation, and coupling), one of the reactance values should be preassigned.

As an example with a preassigned x_{1e}, design procedure for a specified coupling C is described in Fig. 6. Since x_{ee} is a function of C as shown in equation (19), different values of x_{2e} can be calculated from the equation $x_{ee} = x_{1e} + x_{2e}$ with a preassigned x_{1e}. From each value of x_{ee}, the corresponding x_{oo} is determined by equation (17), and $x_{oe} = (x_{1o} + x_{2e})$ is

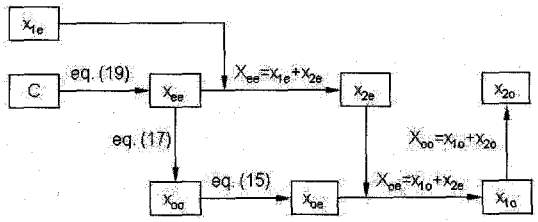

그림 6. 개구면 결합 급전 등진구조 마이크로스트립 방향성 결합기의 설계 흐름도

Fig. 6. Design flow of the aperture-coupled cavity-fed back-to-back microstrip directional coupler.

obtained from the equation (15). Finally x_{1o} and x_{2o} are successively determined. Now the structural dimensions of the directional coupler satisfying these equivalent circuit values should be determined.

IV. Optimized Design

As mentioned before, many structural parameters are involved in the design of the directional coupler studied in this paper. It is known that the equivalent circuit parameters x_{1e} and x_{1o} are functions of the dimensions of coupling section, and x_{2e} and x_{2o} of the connecting stepped impedance line.

At first, the dimensions of cavity and coupling slot such as a, b, t, and L_s should be determined so as to yield the desired x_{1e} and x_1 for the specified coupling power. However, this is not an easy task because many structural parameters involved are linked together. So the optimized design [15] is therefore indispensable, and an evolutionary hybrid optimization method can be efficiently used.

The genetic algorithm (GA) is well known to be one of the powerful global optimization tools for the electromagnetic design problems[4]. This algorithm is particularly effective in the global min-max problems where large numbers of design parameters are involved. However, it is very difficult to find the best solution by applying GA alone due to its statistical property. So it is encouraged to use local optimization algorithms together with GA. The Nelder-Mead method (NM), one of the simplex methods for finding a local minimum of function, is known to be simple and efficient because NM is relied not on numerical

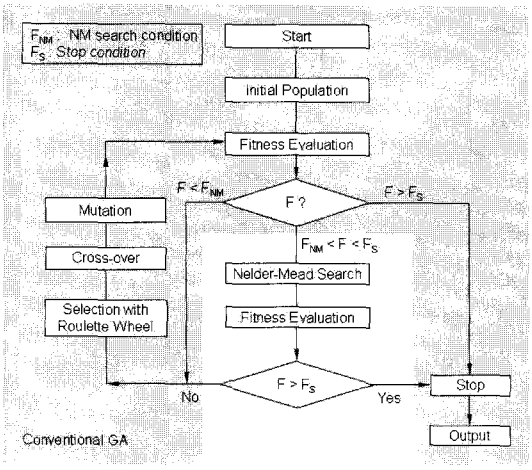

그림 7. 진화적 이동 최적화 방법의 흐름도
Fig. 7. Flow chart of the evolutionary hybrid optimization method.

derivatives (such as Conjugate Gradient) but on a geometrical search[5]. The hybrid optimization algorithm combining GA and NM is therefore chosen for the optimized design of the proposed directional coupler.

The flow chart of the evolutionary hybrid optimization method is shown in Fig. 7. This algorithm starts with an initial set of randomly generated population, which consists of chromosomes whose elements are genes, that is, the structural parameter values to be optimized. In this design example, genes are the dimensions of cavity and coupling slot, and each gene was generated randomly within the appropriate boundary.

Next, the cost and fitness functions are defined and computed for initial population. In general, these are defined as Cost $\geq$ 0 and 0 $\leqq$ Fitness $\leqq$ 1. Since two independent goals of x_{e1} and x_{o1} are involved, the followings are chosen as the cost and fitness functions:

$$\mathrm{COST}=k_1\left(1-\frac{x_{e1}}{(x_{e1})_d}\right)^2+k_2\left(1-\frac{x_{o1}}{(x_{o1})_d}\right)^2 \tag{20}$$

$$\mathrm{Fitness}=\frac{1}{1+k_3\mathrm{Cost}^{k_4}} \tag{21}$$

where $(x_{e1})_d$ and $(x_{o1})_d$ are the desired values of x_{e1} and x_{o1}, respectively. The weighting coefficients k_1 and k_2 should be chosen considering the effect of variations of x_{e1} and x_{o1} on the scattering parameters of the directional coupler, especially on coupling power. And coefficients k_3 and k_4 are chosen the initial fitness distribution to be an appropriate one.

Since the evaluation of cost and fitness will be performed for all population in each generation, the time for this evaluation should be slashed to the minimum within the range of possibility for the efficient design. Quite a decent approach for this aim is to tabularize and store the data of n_t and Y_s for the discrete sets of design parameters a, b, t, L_s in advance for data interpolation.

Since it is difficult to generate population with good fitness values in initial population, reproduction by the GA with crossover and mutation follows after it. Parents for mating are generally chosen by Roulett-Wheel selection. When there are some chromosomes whose fitness values are lager than the threshold value for NM search (F_{NM}) in the repeated process, the NM engine starts to search the much more accurate solutions near these chromosomes. The final step is to evaluate whether the best fitness value meet the stop condition (F_S) or not. If the validity of decision is not sufficient, all steps repeat again up to meet the stop condition.

Next the type and dimensions of connecting line should be determined so as to make x_{2e} and x_{2o} be equal to the obtained values from the design equations. For this aim, a stepped impedance line is a good candidate because arbitrary reactance values x_{2e} and x_{2o} can not be obtained with uniform transmission line. Reactance values of stepped impedance line are given for the corresponding even and odd modes as

$$x_{e2}=\frac{\tan\theta_0-z_1\cot(\theta_1/2)}{1+z_1\tan\theta_0\cot(\theta_1/2)} \tag{22}$$

$$x_{o2}=\frac{\tan\theta_0+z_1\cot(\theta_1/2)}{1-z_1\tan\theta_0\cot(\theta_1/2)} \tag{23}$$

where θ_0 denotes the electrical length of an extended feed line. z_1 and θ_1 are the normalized characteristic impedance and electrical lengths of a stepped impedance line, respectively. In the above system of equations, eliminating $\tan\theta_0$ yields the following quadratic equation of $T_1 = \tan(\theta_1/2)$:

$$cT_1^2 + dT_1 + c = 0 \tag{24}$$

with $c = z_1(1 + x_{e2}x_{o2})$ and $d = (x_{e2} - x_{o2})(1 - z_1^2)$. T_1 can be obtained if z_1 is preassigned. For the practical design, it is encouraged to make the connecting line length be order of quarter-wave length, that is, $\tan(\theta_1/2)$ should be real and positive. This implies that $d^2 - 4c^2 \geq 0$ and c and d should have opposite sign. Now $\tan(\theta_1/2)$ and $\tan\theta_0$, that is, θ_0 and θ_1 can be determined successively under these criterions.

V. Results and Discussions

In order to verify the proposed analysis and design theory, a 10 dB directional coupler was designed. Among the dimensions of cavity and coupling slot, the key parameters a, b, t, and L_s are chosen as the design ones to be determined optimally. The fixed parameters are ε_r = 2.2, h = 31 mils, W_m = 2.40 mm, ε_{rc} = 10.2, and W_s = 0.80 mm. From the given coupling factor of 10 dB, x_{ee} = − 0.7208. If x_{1e} = 1.0000 is preassigned for the design, x_{1o} = 0.3333, x_{2e} = − 1.7208, and x_{2o} = 0.3874 are obtained by Fig. 5 and the design procedure mentioned in Section III.

At first, the design parameters a, b, t, and L_s should be determined so as to yield the desired x_{1e} and x_{o1}. Initially 32 chromosomes were generated, and the maximum generation was set to be 32. In order to find the appropriate values of k_1 and k_2, the effect of variations of x_{e1} and x_{o1} on coupling power was investigated and displayed in Fig. 8. As shown in this figure, x_{e1} affects approximately three times stronger than x_{o1}, k_1 = 0.75 and k_2 = 0.25 were therefore chosen as weighting coefficients. In addition, k_3 = 15 and k_4 = 1.5 were selected for defining the fitness.

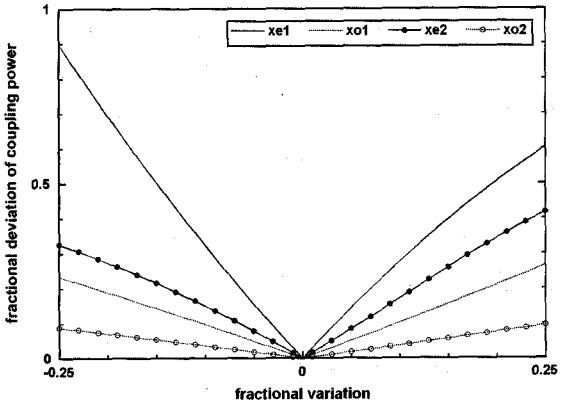

그림 8. 등가회로 소자 값 변화가 결합량에 미치는 영향

Fig. 8. Effect on coupling power of the variation of equivalent circuit values.

표 1. GA 단일 방법과 이종 GA 방법을 통해 얻어진 최적 설계 결과

Table 1. Optimized design results with GA alone and Hybrid GA.

	trial	a	b	t	Ls	cost	fitness	xe1	xo1	S11 (dB)	S21 (dB)	S31 (dB)	S41 (dB)
GA alone	1	22.54	4.45	3.84	10.42	0.002	0.999	0.991	0.347	-49.78	-0.43	-10.29	-58.16
	2	25.21	3.81	18.23	6.43	0.005	0.995	1.005	0.357	-50.58	-0.43	-10.24	-47.56
	3	21.68	3.03	5.38	10.72	0.000	1.000	1.000	0.336	-66.77	-0.45	-10.04	-66.54
	4	27.88	4.72	4.13	10.28	0.022	0.952	0.964	0.377	-38.84	-0.35	-11.11	-49.26
	5	27.90	2.84	5.71	10.52	0.011	0.983	0.948	0.333	-42.44	-0.39	-10.70	-42.37
Hybrid GA	1	22.18	2.54	6.42	10.83	0.000	1.000	1.000	0.333	-87.22	-0.46	-10.00	-87.60
	2	24.30	2.88	5.60	10.75	0.000	1.000	1.000	0.334	-80.13	-0.46	-10.01	-83.60
	3	21.39	2.65	6.13	10.81	0.000	1.000	1.000	0.333	-91.39	-0.46	-10.00	-85.74
	4	25.84	4.62	18.52	5.94	0.000	1.000	1.001	0.332	-66.43	-0.46	-9.96	-74.70
	5	20.12	3.47	4.62	10.62	0.000	1.000	1.000	0.333	-82.62	-0.46	-9.99	-91.08

Thresholds for NM search and stop condition were chosen as F_{NM} = 0.8 and F_S = 0.999, respectively. Table 1 shows the structural dimensions obtained with GA alone and the evolutionary hybrid method, respectively. Stop condition was not met in most of the trials with GA alone even if 32 generations were allowed to be repeated. On the contrary, only average 2-4 generations were needed in the evolutionary hybrid method to meet the stop condition with excellent results. In addition, it did not take much time for NM search in this case.

Next, the dimensions of stepped impedance line was determined so at to yield x_{2e} = − 1.7208 and x_{2o} = 0.3874 by the approach mentioned in Section IV. Since $c > 0$ in this design example,. $d < 0$ should be hold. This implies that z_1 should be preassigned as $z_1 \leq 1$. Now $\tan(\theta_1/2)$ and $\tan\theta_0$, that is, θ_0 and θ_1 can be determined successively. In this paper, θ_0 = 12.12° and θ_0 = 26.03° were obtained for the chosen z_1 = 0.7.

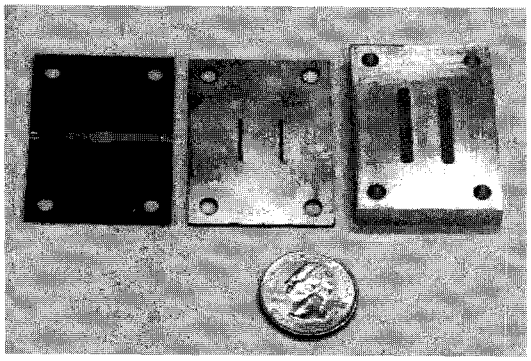

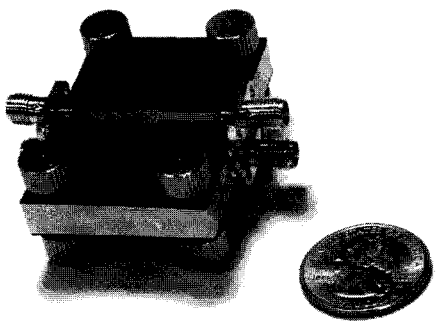

그림 9. 제작된 개구면 결합 급전 등진구조 마이크로스트립 방향성 결합기

Fig. 9. Fabricated aperture-coupled cavity-fed back-to-back microstrip directional coupler

The final structural dimensions obtained by the aforementioned procedure are a = 23.50 mm,, b = 2.54 mm, t = 7.00 mm, and L_s = 12.80 mm., L_{m0} = 2.45 mm, L_{m1} = 5.18 mm, and W_{m1} = 4.00 mm. For the validation check of the design theory, the designed directional coupler was fabricated (Fig. 9), and the measured characteristics are shown in Fig. 10. The measured coupling is 10.3 dB at 3 GHz, and the return loss and isolation are 31.8 dB and 30.5 dB, respectively. Measured coupling variation is ±1.4 dB and ±2.5 dB over 5 % and 10 % bandwidths, respectively. Further studies seem to be needed for reducing the coupling variation for many applications. As shown in this figure, the observed quadrature phase deviation is 1.5° and 2.7° over 5 % and 10 %

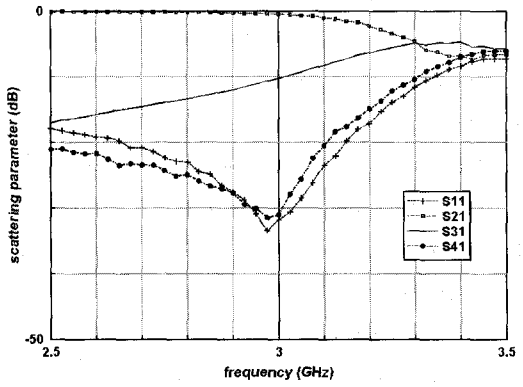

(a)

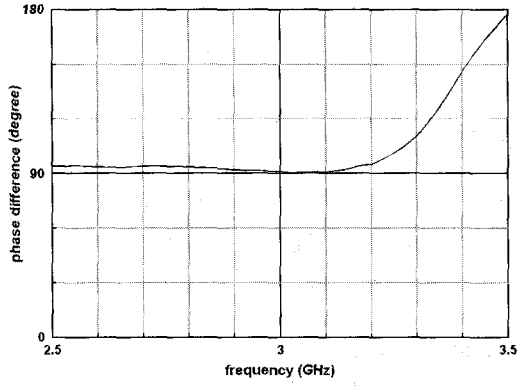

(b)

그림 10. 개구면 결합 급전 등진구조 마이크로스트립 방향성 결합기의 측정 결과;
(a) 산란계수의 크기; (b) S_{21}과 S_{31}의 위상 차이

Fig. 10. Measured characteristics of aperture coupled cavity fed back to back microstrip directional coupler; (a) magnitude of scattering parameters; (b) phase difference between S_{21} and S_{31}

bandwidths. It is shown that excellent quadrature phase characteristics can be obtained from the present directional coupler. The reasonable agreements with the specifications show the validity of the present network analysis and design theory as well as the usefulness of the aperture-coupled cavity-fed back-to-back microstrip directional coupler.

VI. Conclusions

A network analysis and design theory of an aperture-coupled cavity-fed back-to-back microstrip directional coupler was presented for the efficient and optimized design. For this purpose, an equivalent network was developed, and simple but accurate calculation of circuit element values was described. Based on this equivalent circuit, design equations of the coupler were derived and applied to design a 10 dB directional coupler. The hybrid optimization method based on the genetic algorithm and the Nelder-Mead method was invoked to treat several design parameters simultaneously. Good agreements between the measured and the specifications fully validated the proposed network analysis and design procedure.

References

[1] D. M. Pozar, "Analysis and design of cavity coupled microstrip couplers and transitions," *IEEE Trans. Microwave Theory Tech*, vol.51, no. 3, pp.1034 1044, Mar. 2003.

[2] J. Cheng, "A fast hybrid MoM/FEM technique for microstrip line vertical couplers with multiple identical cavities," *IEEE Antennas and Propagation Society International Symposium*, vol. 2, pp. 1076 1079, Jun. 2003.

[3] Eric S. Li, Jui Ching Cheng, and Chih Che Lai, "Designs for broad band microstrip vertical transitions using cavity couplers," *IEEE Trans. Microwave Theory Tech*, vol.. 54, no. 1, pp. 464 472, Jan. 2006.

[4] R. L. Haupt and S. E. Haupt, *Practical Genetic Algorithms*, 2nd ed., Wiley, 2004.

[5] J. A. Nelder and R. Mead, "A simplex method for function minimization," *Computer Journal*, Vol. 7, pp. 308 313, 1965.

[6] J. P. Kim and W. S. Park, "An improved network modeling of slot coupled microstrip lines," *IEEE Trans. Microwave Theory Tech*, vol. MTT 46, no. 10, pp. 1484 1491, Oct. 1998.

[7] J. P. Kim and W. S. Park, "Network Analysis and Synthesis of Multi Slot Back to Back Microstrip Directional Couplers," *IEEE Trans. Microwave Theory Tech*, vol. MTT 48, no. 11, pp. 1935 1942, Nov. 2000.

[8] J. P. Kim and W. S. Park, "Analysis and Network Modeling of an Aperture Coupled Microstrip Patch Antenna," *IEEE Trans. Antennas Propagat*, vol. AP 49, no. 6, pp. 849 854, Jun.2001.

[9] J. P. Kim, "Analysis and equivalent circuit of aperture coupled cavity fed microstrip patch antenna," *Microwave Opt. Tech. Lett.*, vol. 48, no. 5, pp. 843 846, May. 2006.

[10] D. M. Pozar, "A reciprocity method of analysis for printed slot and slot coupled microstrip antennas," *IEEE Trans. Antennas and Propagat.*, vol. AP 34, no.12, pp. 1439 1446, Dec. 1986.

[11] T. Itoh, "Spectral domain immittance approach for dispersion characteristics of generalized printed transmission lines," *IEEE Trans. Microwave Theory Tech, vol.* MTT 28, no. 7, pp. 733 736, Jul. 1980.

[12] E. H. Newmann and D. Forral, "Scattering from a microstrip patch," *IEEE Trans. Antennas Propagat.*, vol. AP 35, pp. 245 251, Mar. 1987.

[13] D. R. Rhodes, "On a fundamental principle in the theory of planar antennas," *Proc. IEEE*, vol. 52, pp. 1013 1021, Sep. 1964.

[14] R. E. Collin, *Foundation for Microwave Engineering*, 2nd ed., McGraw Hill, 1992.

[15] P. Venkataraman, *Applied Optimization with MATLAB Programming*, JohnWiley and Sons, 2002.

저 자 소 개

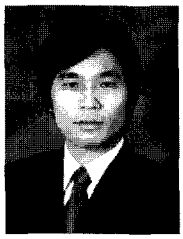

남 상 호(학생회원)
2007년 2월 중앙대학교 전자전기공학부 (공학사)
2007년 3월～현재 중앙대학교 전자전기공학부 석사과정
<주관심분야 : 마이크로파 회로 설계 및 레이더 시스템설계>

남 경 민(학생회원)
2005년 8월 중앙대학교 전자전기공학부 (공학사)
2005년 9월～현재 중앙대학교 전자전기공학부 석사과정
<주관심분야 : 안테나 설계 및 레이더 시스템>

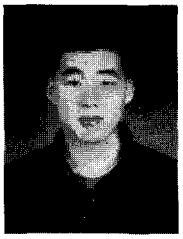

김 철 언(학생회원)
2007년 2월 중앙대학교 전자전기공학부 (공학사)
2007년 3월～현재 중앙대학교 전자전기공학부 석사과정
<주관심분야 :무선통신용 송수신 시스템 및 부품 설계>

장 국 현(학생회원)
2005년 2월 중앙대학교 전자전기공학부 (공학사)
2005년 3월～현재 중앙대학교 전자전기공학부 석사과정
<주관심분야 : 안테나 및 고주파 회로설계 및 레이더 시스템설계>

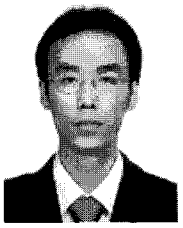

이 장 환(학생회원)
2006년 2월 중앙대학교 전자전기공학부(공학사)
2006년 3월～현재 중앙대학교 전자전기공학부 석사과정
<주관심분야 : 안테나 설계 및 레이더 시스템>

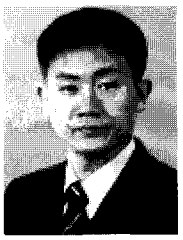

김 정 필(정회원)
1988년 2월 서울대학교 전자공학과(공학사).
1990년 2월 포항공과대학교 전자전기공학과 (공학석사).
1998년 2월 포항공과대학교 전자전기공학과 (공학박사).
1990년 1월～2001년 2월 LG 이노텍(주) 연구소 책임연구원
2001년 3월～현재 중앙대학교 전자전기공학부 부교수
<주관심분야 : 마이크로파 회로설계, 마이크로스트립 안테나설계, 무선통신용 송수신 시스템 및 부품 설계>